SU-SEL-73-022

Recent Results from Satellite Beacon Measurements

by

A.V. da Rosa

June 1973

Technical Report No. 15

Prepared under
National Aeronautics and Space Administration
Research Grant No. 05-020-001

RADIOSCIENCE LABORATORY

STANFORD ELECTRONICS LABORATORIES

STANFORD UNIVERSITY • STANFORD, CALIFORNIA

SEL-73-022

RECENT RESULTS FROM SATELLITE BEACON MEASUREMENTS

by

A.V. da Rosa

June 1973

Technical Report No. 15

Prepared under

National Aeronautics and Space Administration
Research Grant No. NGR 05-020-001

Radioscience Laboratory
Stanford Electronics Laboratories
Stanford University Stanford, California

ABSTRACT

A review is made of the techniques for measuring ionospheric electron content, the most important parameter in the study of transionospheric propagation. Data collected since 1964 have yielded a synoptic description of the behavior of the electron content in midlatitudes. Empirical relationships between the level of solar activity and the electron content have been developed permitting the prognostication of the electron content values. Construction of such prognostication schemes has been stimulated by current efforts to create accurate satellite borne navigation systems. Marked discrepancies between prognostication and observation which occur during ionospheric storms, are being studied to identify their causes. Electron content bite outs during solar eclipses fall off with distance from totality more rapidly than simple theory predicts suggesting the action of eclipse induced neutral winds. Gravity waves propagating in the thermosphere leave a signature in the electron content records. Studies of such records have allowed the identification of the position of the gravity wave source, and its radiation pattern. A one-to-one relationship between these waves and polar substorms has been revealed. Electron content measurements have been used to monitor the protonosphere with good time resolution. Protonospheric storms have been observed with this technique. Slab thickness data obtained from content measurements have been used to determine the neutral air temperature in the thermosphere.

ILLUSTRATIONS

ILLUSTRATIONS

TABLES

The earliest uses of radio beacons aboard satellites date back to the Sputnik ear. Thus, a classical paper on the determination of the ionospheric electron content was written by Garriott[1960] based on data collected from Sputnik III in 1958/59. The first beacons designed for ionospheric propagation studies were placed on low orbiting satellites and yielded a nearly instantaneous picture of the electron content along a given track. Typical satellites of this type were BE-B and BE-C, the former in a high inclination orbit essentially scanning the ionosphere along a N-S track and the latter in a low inclination orbit scanning in an E-W direction. Scientists from all over the world made good use of the availability of these beacons and considerable amounts of data were collected. Although the interest in low orbiting beacons has waned, it has not disappeared. For example, Spain is about to launch its first satellite -- the INTASAT -- which has several of the features of BE-B; in addition, DNA 002 to be placed this year in a circular orbit at 440 km altitude with an inclination of 98.5° will contain a beacon to be used mainly for scintillation studies.

Beacons placed on geostationary satellites have the distinct advantage of permitting the continuous surveillance of a fixed volume of the plasmasphere and for this reason, are much more popular at present. I will confine this paper to results obtained from such beacons.

Use of geostationary satellites for propagation studies began in 1964 when the signals from the VHF telemetry transmitter aboard SYNCOM-III became available. This satellite was parked over the international date line so that only stations in the Pacific area could collect data, a

fact that put the University of Hawaii and Stanford University in a privileged position. These organizations have observed geostationary satellites in an almost uninterrupted manner since 1964 up to the present. Additional impetus to such work was provided by the launching of ATS-1, in 1966. This satellite was also parked over the international date line and substituted SYNCOM-III which had drifted out of range of the West Coast of the U.S. Again, no special equipment was used aboard: the VHF telemetry transmitter served as a beacon. The same occurred with the next two satellites of the ATS series: ATS-3 and ATS-5. These, however, incorporated a simple modification that caused a small amount of the third harmonic of the VHF signal to be radiated, thus effectively acting as a dual frequency beacon useful in protonospheric observations as described later.

The first (and possibly, last) geostationary satellite to be equipped with a specially designed beacon, is ATS-F to be launched in mid-1974. The beacon will emit signals at 40, 140, and 360 MHz, modulated by a 1 MHz tone. The 40 and 360 MHz carriers will also be modulated by 100 kHz. Such a combination of frequencies (all coherent) will allow a wide range of propagation experiments.

Signals from both low orbit and geostationary satellite beacons are used mainly in one of two different propagation experiments: scintillation studies and measurement of electron content.

One simple but significant result of scintillation studies is the discovery that in certain regions of the world, gigaherz signals transmitted through the ionosphere, may suffer strong amplitude and phase

disturbances. This is particularly true in the equatorial and the auroral regions and may have a profound influence on the cost of satellite to ground communication systems: enough additional effective radiated power must be provided to avoid signal loss during deep fading periods. Such behavior came as somewhat of a surprise to engineers and scientists comfortably convinced that the scintillation index was proportional to $f^{-\eta}$, where η was supposed to be about 2. It turned out that the exponent is itself a function of the depth of scintillation and may become a small number or even a negative one. The study of scintillation is, however, one outside my own field, and I will therefore confine this work to the measurement of electron content.

Electron content measurements are based either on the birefringence of the ionosphere or on its dispersivity. The latter can manifest itself by the difference in propagation times of signals of different frequencies or by the fact that the refraction of such signals is not the same. Thus, by observing the different angles of arrival of signals of different frequencies coming from a satellite it is possible to determine the electron content. This technique, at present, does not present advantages capable of balancing the cost of the necessary radio-interferometers.

When two signals of different frequencies are transmitted from a satellite through the ionosphere, they experience different retardations which can be measured by comparing the phases received on the ground. With the usual combination of frequencies (say 140 and 360 MHz, as on ATS-F) absolute values of electron content cannot be directly measured because the difference in retardation is such that the observed phase

differences can be several hundred times 360°, and the resulting ambiguity cannot be simply resolved. On the other hand, this technique is extremely sensitive to changes in electron content. For instance, the 137/412 MHz pair on ATS-3/5 allows the resolution of better than 10^{14} el.m^{-2}. Since on the middle of an equinoctial day, during sunspot maximum, the slant electron content can be some 10^{18} el.m^{-2}, a resolution of better than 1:10^{4} can be obtained. The question of determining the absolute value of electron content from this so-called phase-path difference technique was resolved a long time ago for the case of low orbiting satellites (Mendonça[1962]) but only recently for the case of geostationary ones (Almeida[1972]). The method employed with geostationary satellites is a hybrid one and uses information from Faraday rotation measurements. An uncertainty of less than 10^{16} el.m^{-2} can be achieved.

The equipment used in the phase-path difference method consists of phase-locked receivers and is, therefore, expensive and not very appropriate to unattended operation. These disadvantages, together with the difficulties in the determination of the absolute value of electron content, led workers in this field to the idea of the "group delay experiment". In this case, the phases of the modulation envelope of two carriers at different frequencies are compared. In the case of ATS-F, for instance, the phases of the 1 MHz envelopes of either the 40 and 140 MHz carriers can be compared with that of the 1 MHz modulation envelope on the 360 MHz carrier. Since the wavelengths involved are much larger than those used in the phase-path difference method, the ambiguity now

TABLE 1

f_m \ f	40	140	MHz
0.1	12 ±0.3	170 ±5	$\leftarrow I_A$, $\leftarrow I_U$
1.0	1.2 ±0.03	17 ±0.5	$\leftarrow I_A$, $\leftarrow I_U$

MHz

$m^{-2} \times 10^{-16}$

Table 1. ATS-F Group Delay Experiment. Ambiguities (I_A) and uncertainties (I_U) in the measurement of electron content using either 40 or 140 MHz signals in conjunction with the 360 MHz reference signal. Two modulation frequencies are considered: 0.1 MHz and 1 MHz.

is also much larger and can be resolved easily. Table 1 shows the ambiguities and uncertainties of the group delay experiment on ATS-F. Uncertainties are based on a conservative estimate of ± 10' uncertainty in the phase angle measurement. One basic assumption in this experiment is that the relative phase of the modulation envelopes of the signals as they leave the satellite is known. This is a crucial question mark in the experiment.

By far the most popular method of determining the ionospheric electron content is that based on the measurement of the Faraday rotation of a linearly polarized signal, in general, at VHF. The great advantage of this method is the simplicity of the equipment both on the ground and on the satellite. The latter may simply be an existing VHF telemetry transmitter: one or two watts of effective radiated power being sufficient. On the ground, the most commonly used equipment is one employing a mechanically rotating Yagi antenna, developed by Prof. John Titheridge of New Zealand. Recently more sophisticated VHF polarimeters, using fixed antennas, appeared on the market.

The main drawbacks of the Faraday rotation method are the substantial uncertainties associated with the conversion of Faraday rotation angle into electron content values and the fact that the method becomes progressively less sensitive as the observation site moves closer to the geomagnetic equator.

Adequate electron content information has been accumulated over the last few years by stations in or near New Zealand and by those in the U.S. (including Hawaii and Puerto Rico). Other areas of the world are

not as well covered. Figures 1,2, and 3 show typical results. The collected data have been put to good use on both science and engineering.

The increasing use of transionospheric transmissions between earth and artificial satellites or other astronomical bodies is generating a growing demand for better knowledge and more accurate predictions of the behavior of the electron content of the plasmasphere.

With the proliferation of geostationary satellites, communications engineers require knowledge of the maximum bandwidth that can be transmitted through the ionosphere with a tolerable phase distortion. This dispersive nature of the medium may cause the bandwidth to be limited by the electron content; the maximum bandwidth is then a function of the time of day, the season of year, and the phase of the solar cycle. A related problem, also dependent on the value of the electron content, is the question of the distortion suffered by short pulses transmitted through the ionosphere.

Efficient launch operations of some satellites as well as accurate position keeping of satellites already in orbit require the determination of the spin-axis orientation with a precision of about 0.1°. This can be done by measuring the polarization angle of a wave radiated from a satellite antenna mounted along the spin-axis. To obtain the desired accuracy, it is imperative that the Faraday rotation in the plasmasphere be taken into account.

The transmission of time signals via satellites offers definite advantages over the use of HF but again, for the highest accuracy, transmission delays due to the electron content must be taken into account.

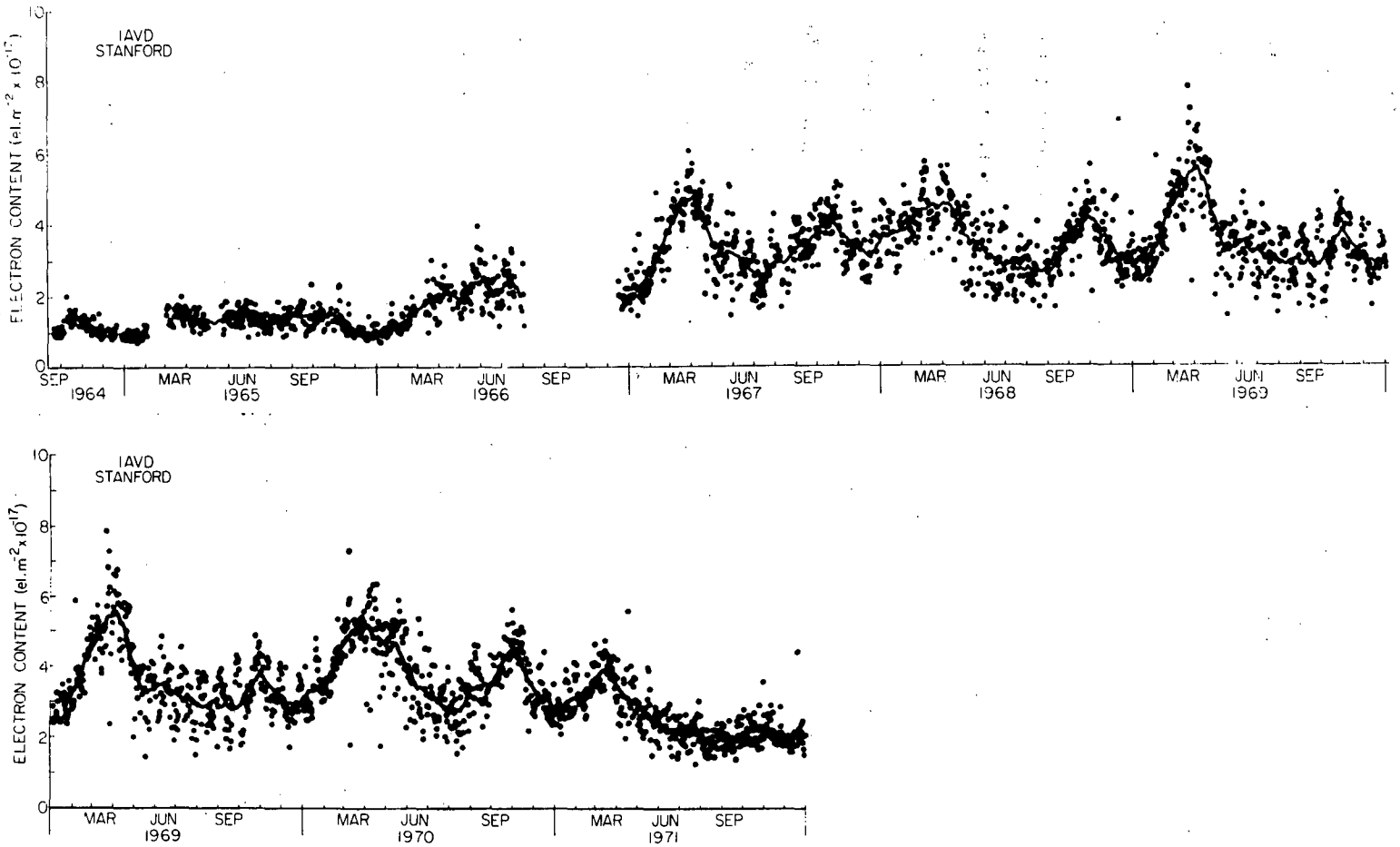

Figure 1. The daytime average value of electron content (0900 to 1500), IAVD, for Stanford. The solid line is a 31-day running mean through the data. SYNCOM III observations were used up to July 1966 and ATS-1 observations began on the last days of that year.

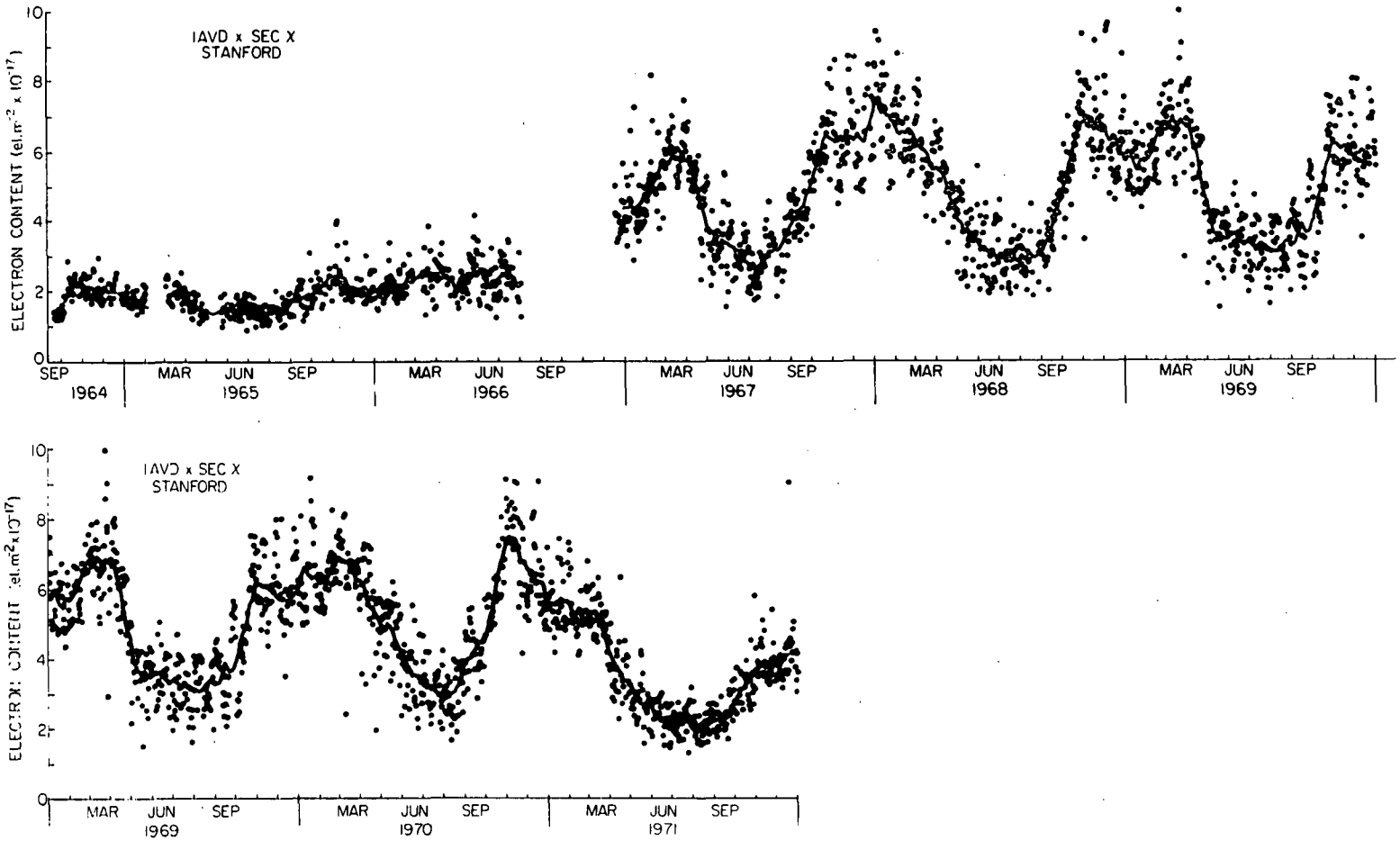

Figure 2. The data of Figure 1 are plotted with a correction for an overhead sun.

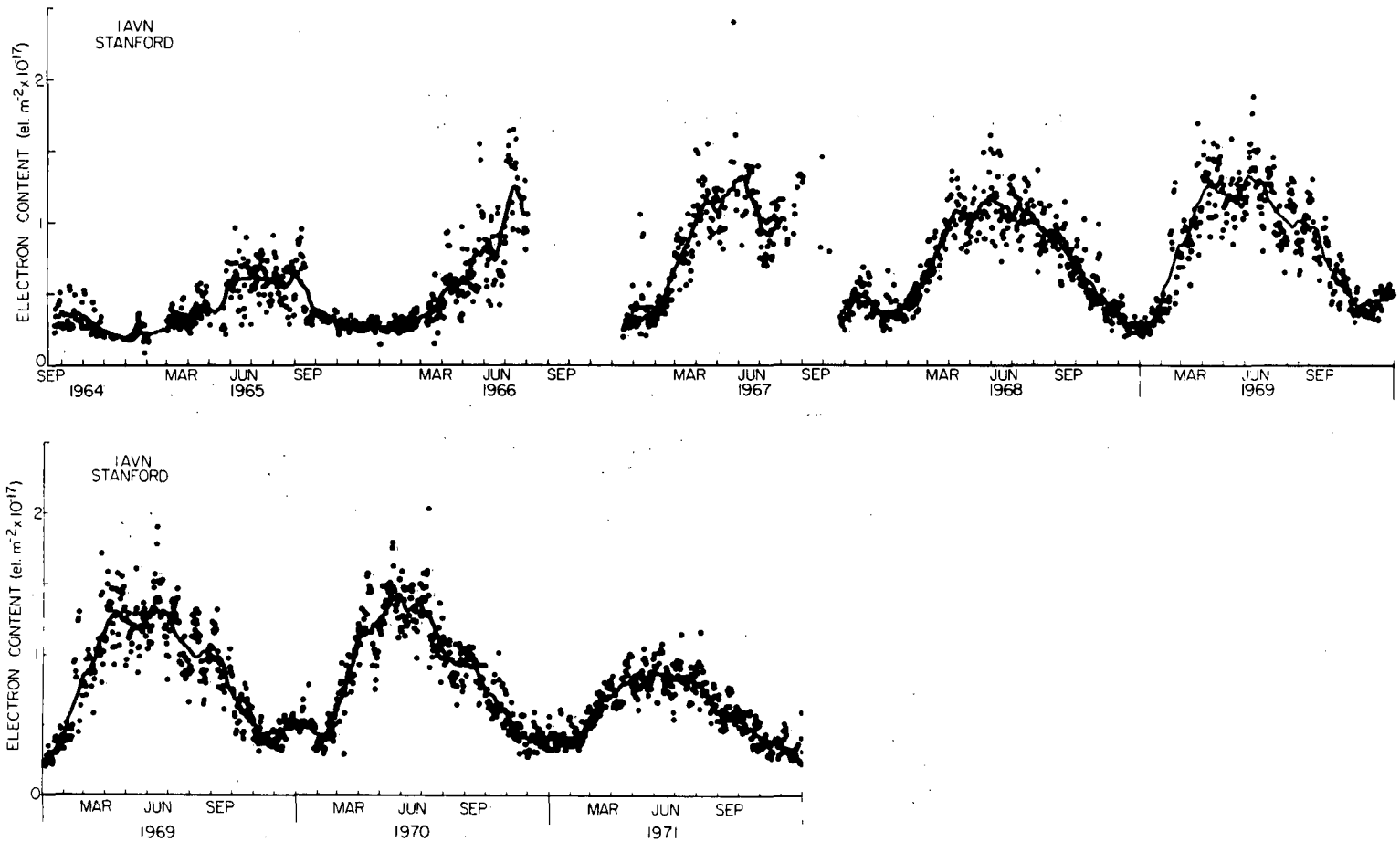

Figure 3. The nighttime average value of electron content (2100 to 0300).

The capacity of communications channels between a satellite repeater and ground can be doubled by using polarization separation of two transmissions employing the same frequency. To accomplish this, orthogonal, linearly polarized antennas are used, and it is necessary to compensate for the Faraday rotation in the ionosphere when orienting the ground antennas. Predictions of the expected Faraday rotation are very useful in designing the system.

Perhaps the most acute need for good ionospheric data comes from the people who are developing precision navigation systems. The one system that seems to be more advanced in its development is the DNSS (Defense Navigation Satellite System) of the Department of Defense of the U.S. This system employs a constellation of four geo-synchronous satellites, one of which is geostationary while the other three are placed in such an orbit that their ground track is a circle of some 30 geographical degrees in diameter centered on the subsatellite point of the geostationary spacecraft. The three coordinates of the user (latitude, longitude, and altitude) are determined by ranging measurements to the satellites. Four, instead of three, satellite to user distances have to be measured because additional information is needed for the synchronization of the user's clock. Thus, with four measurements, the four unknowns -- x, y, z, and vt -- are determined. To obtain t, v has to be known from independent information, and since the mean propagation velocity depends on the electron content in the intervening medium, the latter must be known. One should point out here that there is a requirement that the user be passive, otherwise the capacity of the sys-

tem would be severely restricted. If the user were able to interrogate the satellite then there would be no problem of user clock synchronization.

As the system is to have a precision of a few meters, uncertainties in ionospheric delay become important even at the L-band frequencies used. For this reason considerable effort has been dedicated to the analysis of the ionospheric effects on the accuracy of the system and on finding methods to reduce the propagation uncertainties.

Several organizations have constructed electron content prognostication schemes. Since CCIR has developed tables of coefficients that permit the estimation, on a worldwide basis, of values of f_0F2 (and consequently of N_{max}) given time of day, day of the year, degree of solar activity, and geographic position, and since there is a relationship between the electron content, I, and N_{max}, some of the schemes use the CCIR tables as a starting point.

This requires knowledge of the behavior of the slab thickness, τ:

$$\tau \equiv \frac{1}{N_{max}}$$

An auxiliary prognostication scheme has to be created to estimate τ. This has been done by the Air Force Cambridge Research Laboratories (Klobuchar[1970]) using observed values of I and N_{max}. The University of Illinois (Rao et al.[1971]) used real time electron content values and predicted N_{max} to obtain an estimated slab thickness. This value of τ is then used at a second location together with predicted N_{max}

to prognosticate the electron content. The scheme developed by the Applied Physics Laboratory uses the predicted values of N_{max} in conjunction with theoretically derived slab thickness values, to obtain I.

DBA Systems, Inc., derived its prognostication of τ from worldwide top and bottom side soundings (Bent et al.[1972]). It is the only scheme, at present, that can be applied worldwide.

To avoid the accumulation of errors resulting from the need to prognosticate two quantities (τ and N_{max}), Stanford University (Waldman et al.[1971]) developed a scheme in which the electron content is directly prognosticated from its historical behavior in a manner similar to that used in deriving the CCIR coefficients for f_0F2. The disadvantage of such a method is the present dearth of data that limits the coverage to North America and Hawaii.

Since the r.m.s. accuracy of all proposed schemes is about the same at present, (except for the one of Illinois which appears to be more precise), we will look at some of the Stanford results.

Figures 4,5, and 6 compare the observed diurnal curves of electron content with those predicted by the prognostication scheme and with the 31-day mean curve.

In Figure 4 one can observe a good agreement between observation and prognostication. The 30-day mean is somewhat too high owing to the fact that the 30-day mean solar activity was higher than the activity on the day under consideration. Figure 5 again shows good agreement between observation and prognostication. In this case, however, the mean is too low because the solar activity in the day in question was much

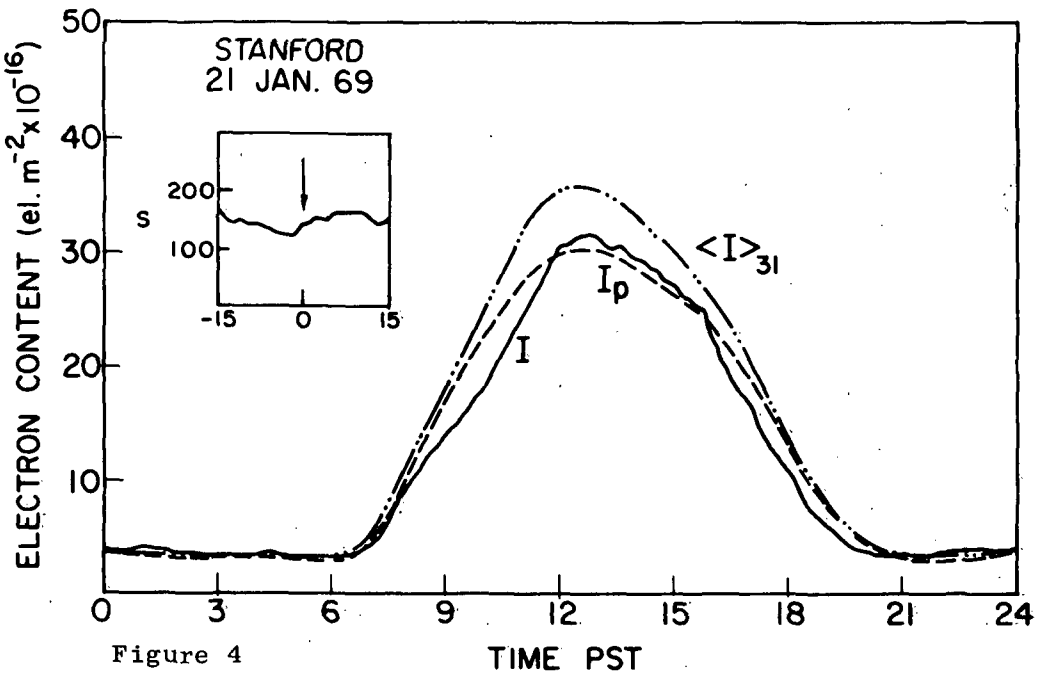

Figure 4

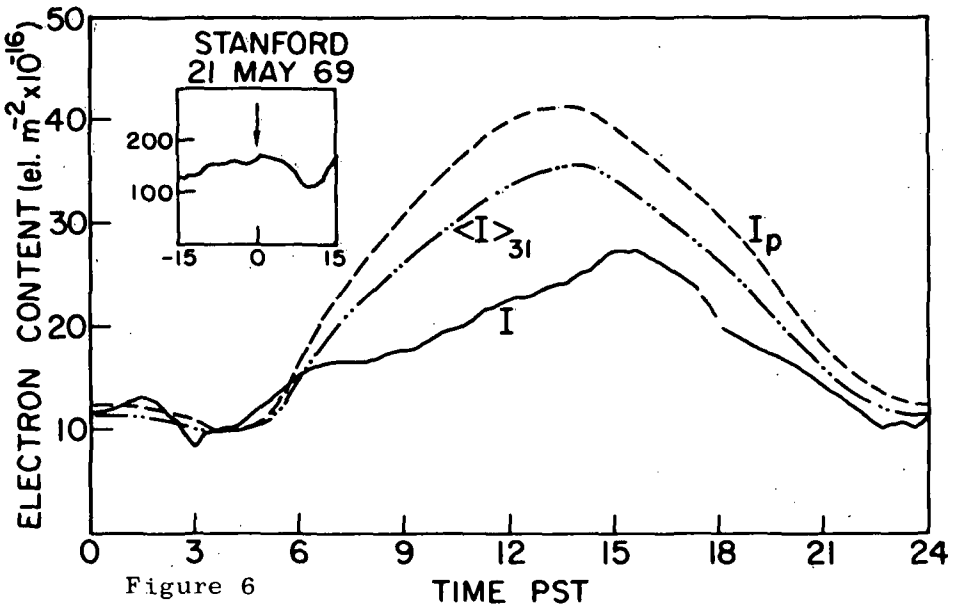

Figure 6

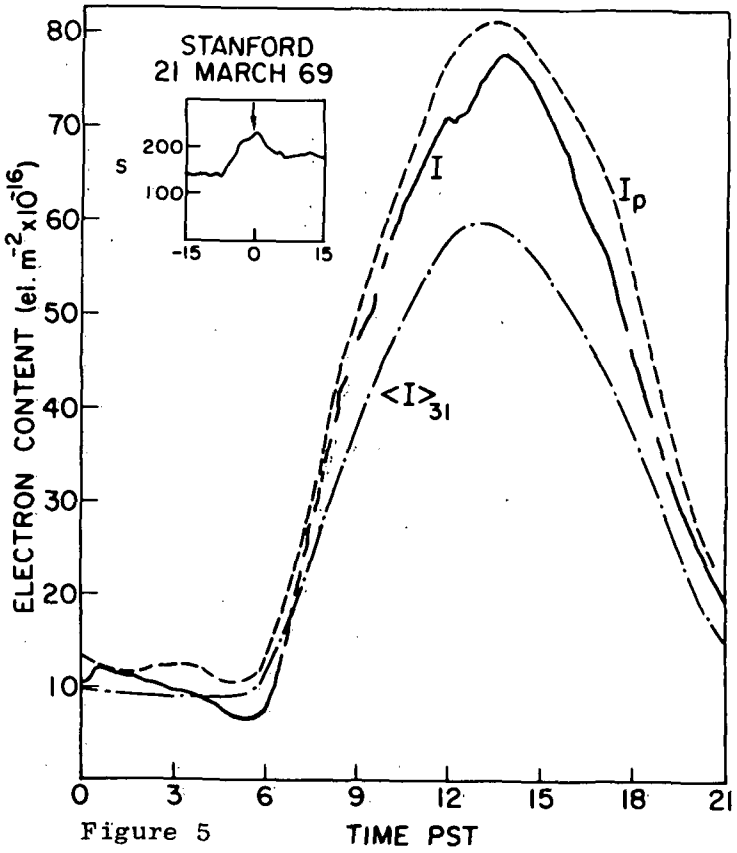

Figure 5

Figures 4,5, and 6. Comparison between the observed electron content (I), the prognosticated value (I_p) and the 31-day mean value I_{31}. Note that the ionospheric storm on 21 May 1969 caused a severe failure of the prognostiation scheme.

higher than the mean. Figure 6 shows a case in which prognosticated values depart drastically from observation owing to an (unpredictable) ionospheric storm.

From the above it can be seen that, although statistically the prognostications may be good, on any given day a serious error may be made.

Hoping to ameliorate the above situation, the idea of supplementing the prognostication by some updating method was introduced. This requires near real time observation of electron content followed by geographical and temporal extrapolation. Clearly such a scheme can only succeed if there is substantial correlation between the behaviors of the electron content at the user and at the observer. In Figure 7, σ_1/σ represents the error reduction or amplification factor resulting from updating, for various values of ρ. Clearly ρ is unknown to the operators of the system. It can be seen that there is an improvement only if $\rho > 0.5$. Otherwise updating will increase the prognosticated error. For this reason, it becomes of interest to study the degree of correlation of the ionospheric electron contents at two points. Figure 8 shows that for stations separated some 700 km and at roughly the same latitude the correlation coefficient during most of the day can be very high, thus permitting effective updating. On the other hand, in Figure 9, the correlation coefficient between Hawaii and Stanford is seen to be always insufficient to permit improvement by updating.

Table 2 summarizes the results obtained with the Stanford prognostication scheme. Four different ranging uncertainties (at 1.6 GHz) are shown. These are r.m.s. uncertainties over the whole period indicated

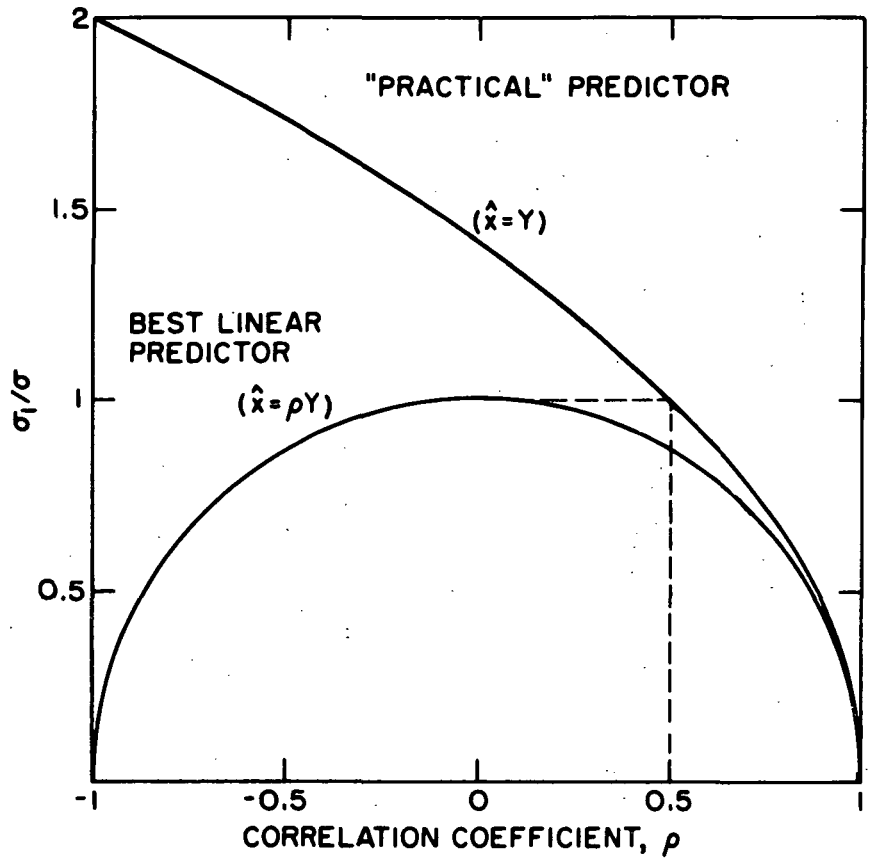

Figure 7. The estimation error reduction (or amplification) σ_1/σ, given by the best linear predictor and a "practical" predictor is shown as a function of the correlation coefficient ρ. When $\rho > 0.5$, both predictors provide error reduction and there is little advantage in using the best linear predictor; when $\rho < 0.5$ the "practical" predictor should not be used because it increases the error rather than diminishing it.

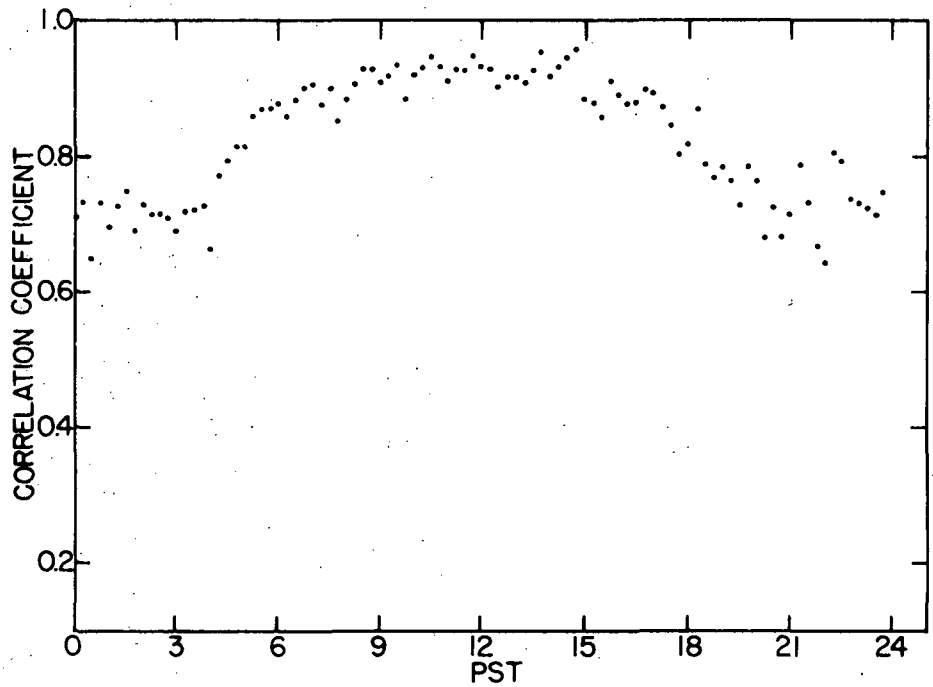

Figure 8. Correlation between electron content values at Ely, Nevada, and Stanford, California, a distance of 700 km. A 30-day interval beginning on day 40 of 1967. Same local time at the two stations.

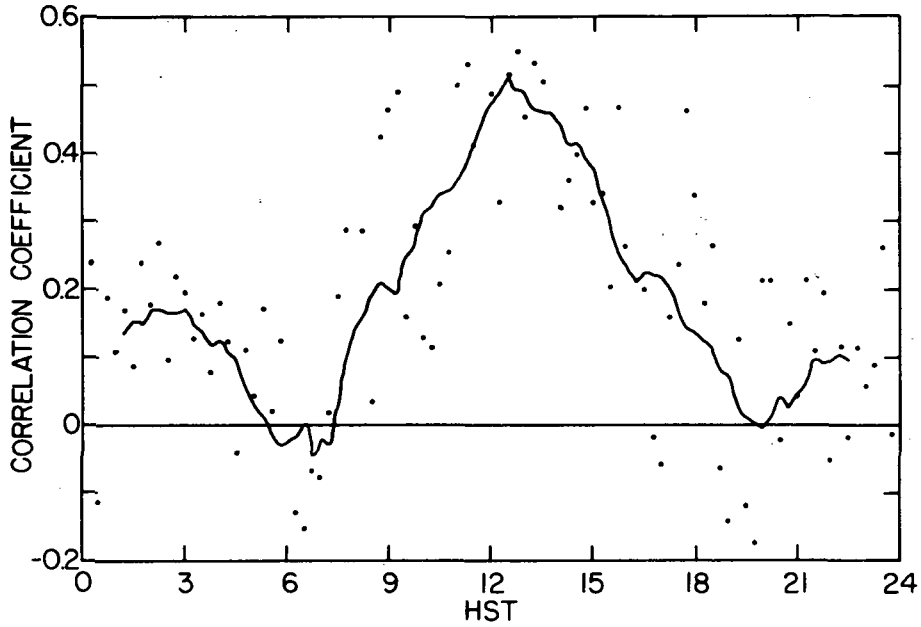

Figure 9. Correlation between electron content values at Honolulu, Hawaii, and Stanford, California, a distance of 4000 km. A 30-day interval beginning on day 40 of 1967. Same local time at the two stations.

TABLE 2

PROGNOSTICATION ERRORS RESULTING FROM THE USE OF DIFFERENT SCHEMES

A PREDICTION AT	B PREDICTOR FROM	DIST. km	PERIOD	ϵ_1	ϵ_2	ϵ_3	ϵ_4
				METERS			
Stanford (1)	Stanford (2)	670	1 JAN 68/31 DEC 68	0.34	0.35	0.46	3.75
Stanford (2)	Stanford (1)	670	1 JAN 68/31 DEC 68	0.34	0.35	0.57	3.94
Edmonton	Ft. Collins	1420	1 DEC 68/13 NOV 69	0.30	0.43	0.31	3.00
Ft. Collins	Edmonton	1420	1 DEC 68/13 NOV 69	0.34	0.44	0.30	3.36
Stanford (1)	Hawaii	3830	1 JAN 65/31 DEC 65	0.23	0.96	0.19	1.26
Hawaii (3)	Stanford (1)	3830	1 JAN 65/31 DEC 65	0.39	1.04	0.25	2.27
Arecibo	Stanford (1)	5910	8 DEC 67/18 APR 68	0.57	0.85	0.23	1.13

Table 2. Summary of r.m.s. residual ranging uncertainties (at 1.6 GHz) when different electron content estimation schemes are employed. See text for explanation of ϵ_1 ... ϵ_4.

in the table. ϵ_1 is the error in the prediction algorithm being tested, i.e., the residual uncertainties after prognostication and updating. ϵ_2 is the error resulting from the simple assumption that the electron content at the prediction location is the same as that at observing location. ϵ_3 is the error when prognosticated values are not updated. ϵ_4 is the error incurred when ionospheric effects are completely ignored. ϵ_4 is equal to several meters and is considered unacceptable for many applications. When the user is not too far from the observing site, ϵ_1 and ϵ_2 are comparable to one another and are smaller than ϵ_3. This means that for short distances, especially if the two sites are at nearly the same latitude, it makes no difference whether one uses the proposed algorithm or simply assumes that the electron content at the user is the same as at the observer. When the user is far from the observer, updating tends to degrade the results: the best is use prognostication with no correction. At intermediate distances, ϵ_1 and ϵ_3 are comparable and are the smallest errors. In such cases it makes little difference whether the algorithm is used with or without updating.

The fact that present prognostication schemes fail drastically on some occasions, indicates that our knowledge of the different processes that influence the ionosphere is still incomplete. Thus, we do not understand the reasons for the large observed day-to-day variations in the ionospheric electron content, the mechanisms that cause ionospheric storms are not clearly grasped, and even the seasonal behavior of the electron content is not satisfactorily explained although several theories have been advanced. Clearly, the solar ionizing radiation is one of the

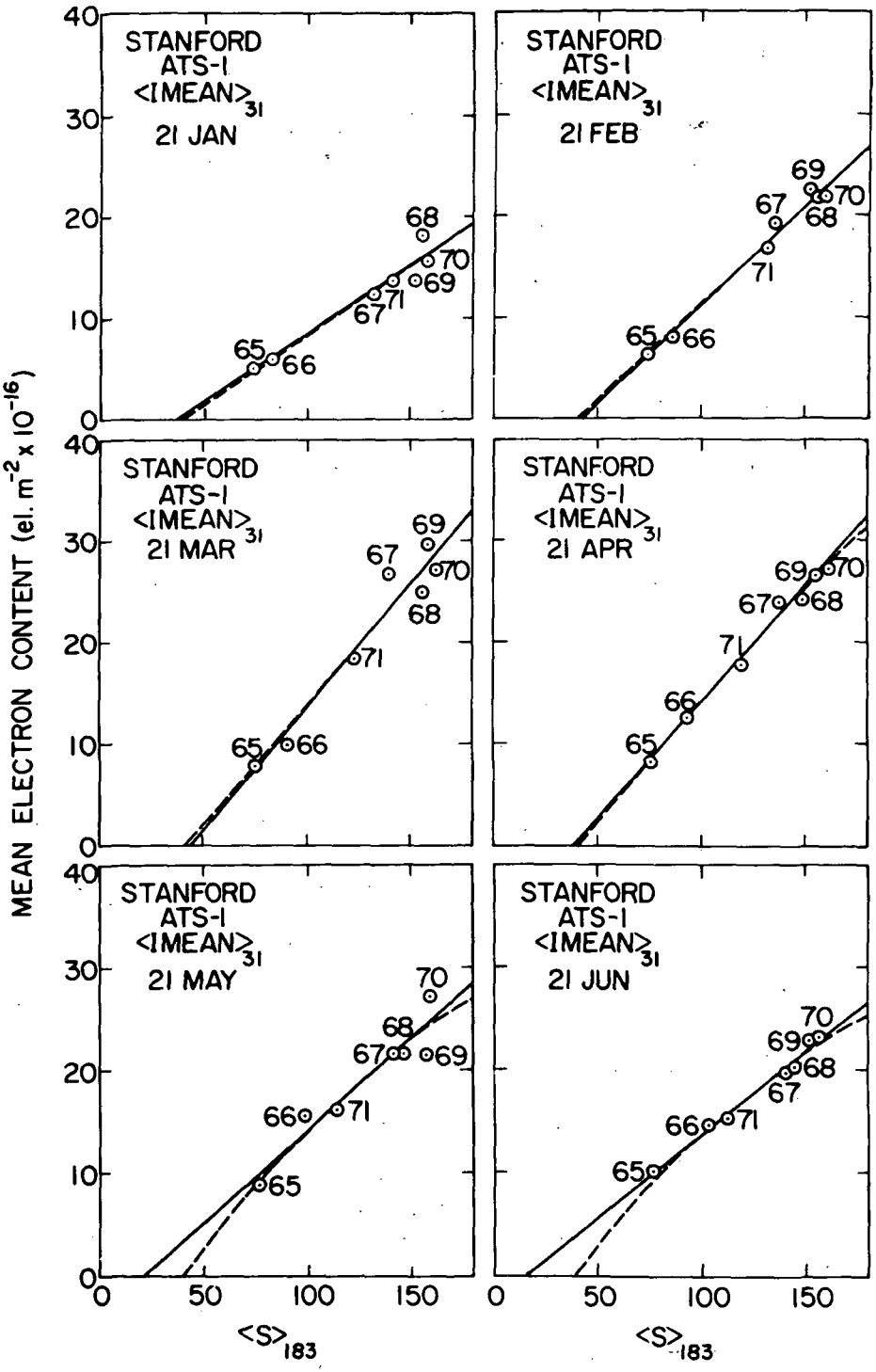

Figure 10. Examples of regression between solar radio flux (S) and daily mean electron content (IMEAN).

driving forces that control our plasmasphere and one that is reasonably well understood. It would therefore be instructive to remove from the observed behavior of the ionospheric electron content, that component that is due to changes in solar EUV: the residual variations in electron content will then contain the effect of all other agencies (or would if all processes were linear). One difficulty with this approach is the fact that we do not have good continuous observations of the EUV spectrum and must instead, rely on an indirect index of solar ionizing radiation: the solar radio flux at 2.8 GHz.

Scatter diagrams of electron content over Stanford versus solar radio flux were prepared covering the period 1964-1971 and a linear regression was determined for every third day (Figure 10). Under the assumption that the short term response of the ionosphere to fluctuations in solar radiation is the same as the long term response, it is possible to write an empirical expression for the daily average value of electron content, IMEAN, in terms of the level of solar radio noise, S:

$$\text{IMEAN} = I_o + \sigma S$$

where I_o and σ depend on the day of the year but not on the level of solar radiation.

Given daily values of S it is then possible to estimate IMEAN. Figure 11 shows the predicted (solid line) and the observed (crosses) values of electron content for 1969. It can be seen that the general trend of the prediction is correct but that there are many marked dis-

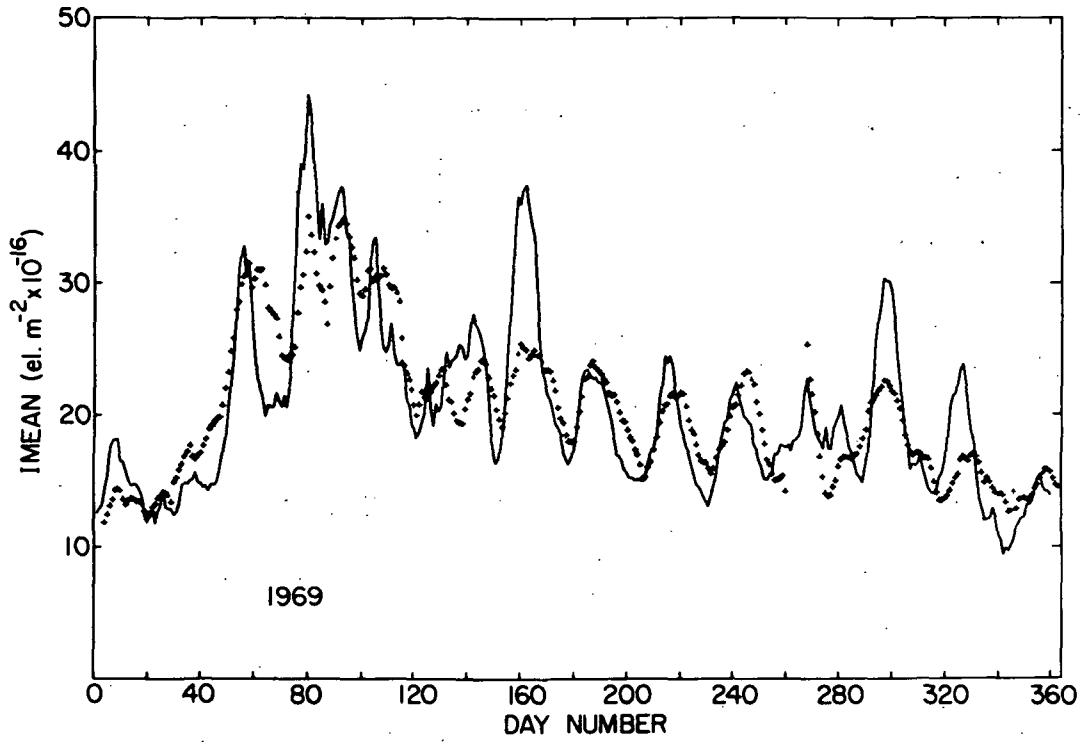

Figure 11. Comparison between predicted (solid trace) and observed values of daily mean electron content (crosses). Data for Stanford ATS-1.

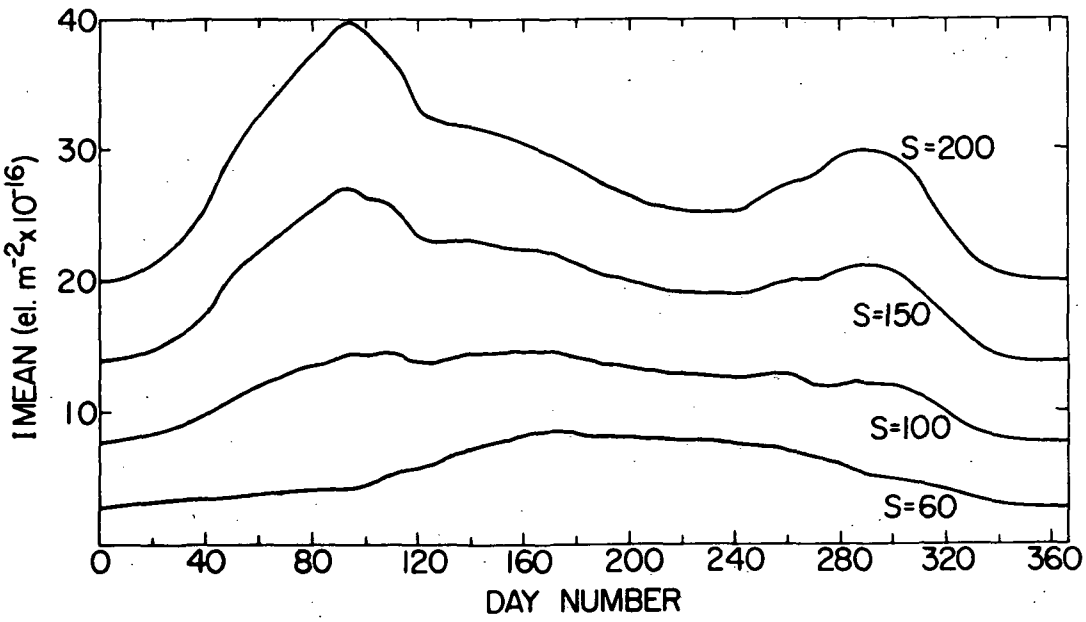

Figure 12. Seasonal behavior of the daily mean electron content.

crepancies whose cause is not known.

It is also instructive to examine what happens when one assumes that throughout a year the sun's activity is constant: this will bring out the seasonal behavior shown in Figure 12. At low solar activity (S = 60) there is more ionization in the summer than in the winter, by just the amount one would expect based on the smaller zenithal angle and longer days in the summer. As the solar activity goes up, equinocial humps begin to appear, the vernal one being more pronounced than the autumnal. Waldman[1971] has proposed an ingeneous explanation for this phenomenon based on the variation of neutral hydrogen content in our atmosphere.

The influence of neutral winds on the degree of ionization in the plasmasphere has been recognized by theoreticians (cf. King and Kohl [1965]) and more recently has been used as explanation for a number of features in the behavior of the ionosphere. The most obvious effect caused by the winds is the action of its meridional component in lifting (equatorward wind, at night) or lowering (poleward wind, at daytime) the ionization and thus altering the average recombination rate. This effect is similar to that caused by electric fields and the question arises which of these two causes is the dominant one. Stubbe[1970] showed that in a quiet day winds are the clearly dominant. On a disturbed day, electric fields are greatly enhanced and override the wind effect. These facts are important when one wishes to examine the wind effect on observed electron content: one must select quiet days.

A recent study of wind effects was made by Bendito[1973] who

analyzed the interesting feedback mechanism that exists in the plasmasphere:

Let us fix our attention to the conditions prevailing during midday when the neutral winds are essentially poleward and tend to depress the ionization. Consider a step increase in solar radiation. The production of ionization will increase almost simultaneously and will quickly result in an increase in electron content. Since in the F-region (which is the main contributor to the electron content) the main restraining force for neutral winds is the ion drag, the increase in ionization will cause a decrease in the average recombination coefficient. This causes the ionization to grow further in a positive feedback loop that searches a new equilibrium point in which h_{max} is substantially higher. After some time delay (Herman and Chandra[1969]) the neutral atmosphere reacts to the increased solar radiation by an increase in temperature. This causes a reduction in the pressure gradients per unit mass that drive the wind so that there is another increase in the electron content.

The conclusion of Bendito's analysis is that the wind effect will cause a relative increase in electron content larger than the relative increase in solar radiation that triggered the changes. In addition, a time delay in the ionospheric response to solar changes is predicted. Experimental observations made during quiet periods in which the solar energy had sufficiently well marked changes, confirms the theoretical predictions. Figure 13 shows the cross correlation function between electron content at Stanford and solar radio noise. It can be seen that

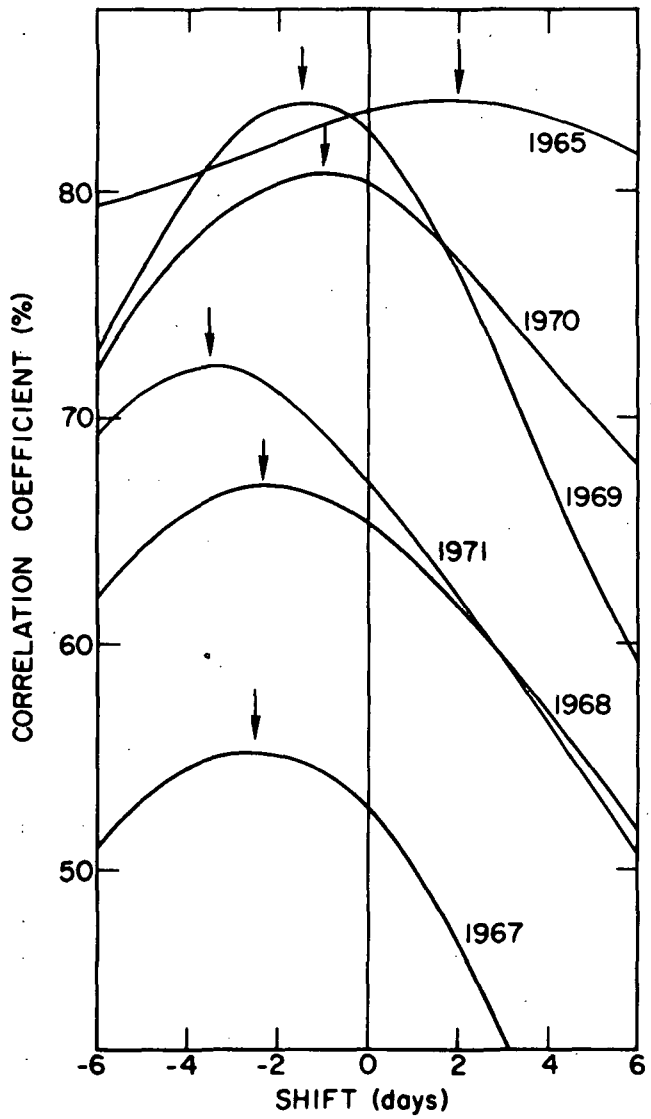

Figure 13. Cross-section between electron content and solar radio flux showing that the content lags by about 2 days (1965 results have no significance. See text.)

for all years, except 1965, the electron content changes lag the solar activity. In 1965, the fluctuations in solar activity were too small to permit any significance to be attached to the cross correlation.

Wind effects on the ionosphere can also be detected by observing the response of the electron content to solar eclipses. Figure 14 shows the 25% bite out in electron content observed at Eastville, VA, USA,

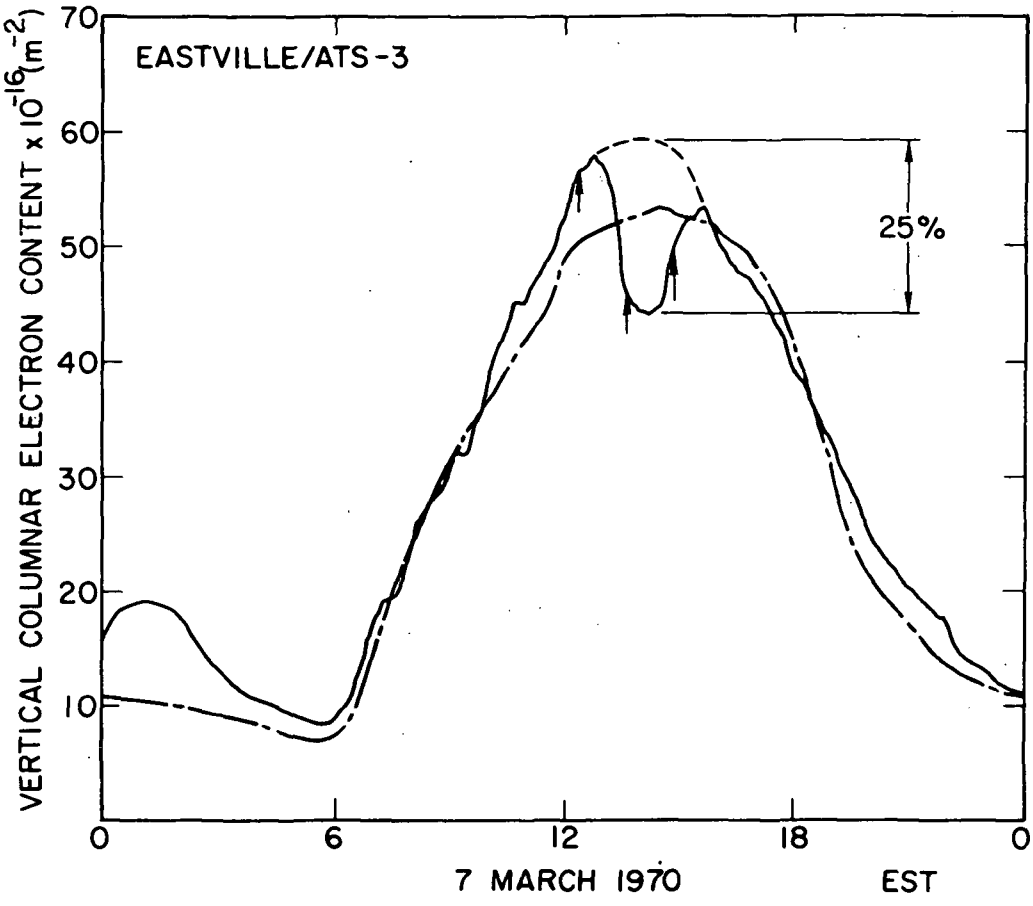

Figure 14. Electron content bite out during the solar eclipse of 7 March 1970, observed in the path of totality.

during the 7 March 1970 solar eclipse. The volume of the plasmasphere under scrutiny was in the path of totality. Simultaneous observations of electron content made at stations in which maximum obscuration of the sun was 45%, showed non-detectable bite outs. This lack of reaction can be explained by postulating a neutral wind flowing towards the volume of the atmosphere cooled by the sun's shadow (Almeida et al.[1972]).

An interesting use of electron content data is made by workers dealing with gravity waves. Such waves leave signatures in electron content records in the form of bumps. Davis[1971] using a four station

network measured the vector velocity of these gravity waves and observed a systematic diurnal oscillation in the travel direction. Average direction was equatorward along the magnetic meridian but a diurnal swing of ± 20° was clearly detectable. This suggested a source in the auroral oval at a fixed geomagnetic time. As the earth spins, the source moves eastward causing the change in direction. Davis was able to pin down the position of the source in the evening sector of the oval and to establish a one-to-one relationship between polar substorms and individual bumps in electron content. Substantial contributions to the understanding of the gravity wave generation and propagation mechanism were made.

Titheridge has recently been able to use a combination of electron content and f_0F2 data to determine the temperature of the neutral atmosphere in roughly the 400 km altitude region. Based on theoretical considerations, a linear relationship between slab thickness and neutral temperature was derived:

$$\tau = \tau_o + \alpha T_n$$

in which α hovers between 0.220 and 0.225 and τ_o depends on season and time of day and has values between 2 and 22 km. Calculated nighttime values of T_n agree with satellite drag values to within ± 5%. Behavior of daytime values resembles more that of values derived from incoherent backscatter. If further investigation along the lines described above consolidate our confidence in this method of temperature measurements,

then a useful tool has been developed for the study of atmospheric processes.

As pointed out in the beginning of this report, electron content measurements of the protonosphere have been carried out by Almeida. This is done by using a combination of phase-path difference and Faraday rotation measurements; the former yields the total electron content, I, up to the satellite while the latter measures essentially the integral:

$$I_F = \frac{1}{B_{LI}} \int_o^S N B_L \, ds$$

where the electron concentration N is weighted by the longitudinal component of the geomagnetic field. Thus the difference between I and I_F can be written:

$$I_W \equiv I - I_F = \int_o^S N(1 - \frac{B_L}{B_{LI}}) ds \equiv \int_o^S N W \, ds$$

Clearly, if W has the property of being equal to zero up to a given height and unity above that height, then I_W is a measure of the electron content above that height. It turns out that for certain geometries of observation, the weighting function W behaves in a manner acceptably close to the ideal one mentioned above, as can be seen in Figure 15. Under such conditions it is possible to observe, on a continuous basis and with good time resolution, the protonospheric content. Results are shown in Figure 16 which display the depletion of the protonosphere following a storm and its eventual build up to normal values. The

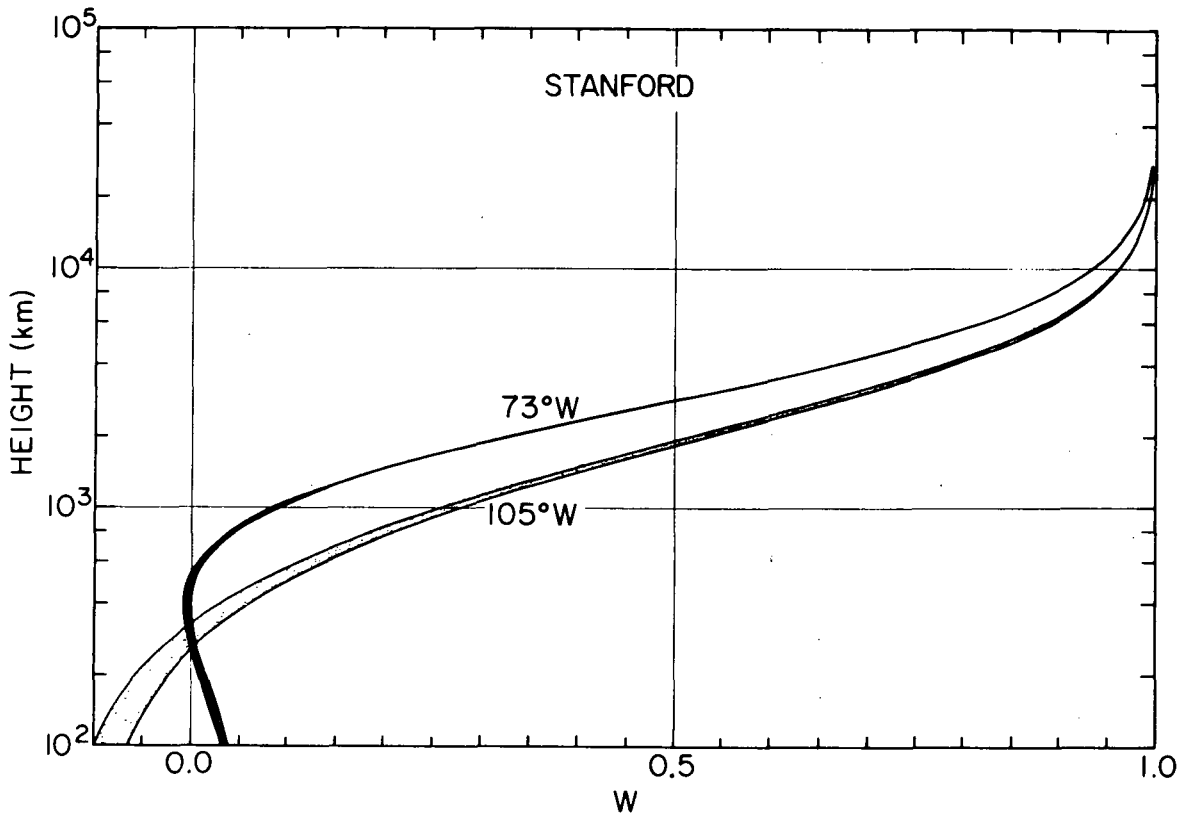

Figure 15. Plots of the weight function W versus height for an observer at Stanford. Two families of W are shown corresponding to geostationary satellites positioned at 73° W and 105° W.

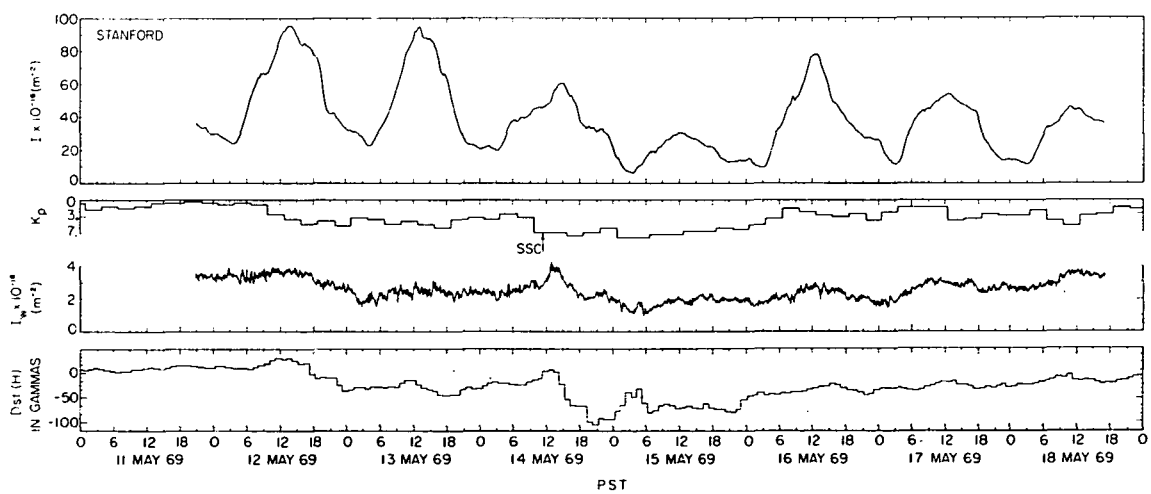

Figure 16. Protonospheric electron content observation, during an uninterrupted period of 7 days in May 1969, from Stanford. The geostationary satellite was parked at 73.4° W.

sharp bump on 14 May 1969 has been interpreted as the signature of a "blob" of plasma peeled off from the protonosphere by the storm enhanced dawn-to-dusk electric fields and ejected into the interplanetary space.

As pointed out when prognostication schemes were discussed, there are a number of days during the year when the electron content behavior departs markedly from the expected. These are, by definition, ionospheric storms, whose close association with geomagnetic storms was recognized early.

Although ionospheric storms can easily be recognized from the examination of ionosonde or Thomson scatter records, the electron content is by far the simplest and most direct way of observing this phenomenon. This is specially true when modern polarimeters are used, yielding real time electron content plots. Figure 17 is a plot of observed electron content (solid line) compared to the 7-day average (dotted line, taken as reference) and shows a typical ionospheric storm. The numbers that appear in the figure are a "disturbance index, D" defined as the ratio (in percentage) of the mean quadratic deviation of electron content from its average to the average value. Day 81 is seen to be essentially undisturbed (D = 6%). The storm starts on day 82 and is characterized by an enhancement of electron content followed eventually by a depression and a subsequent recovery.

Examination of electron content records shows that the behavior of this quantity is strongly dependent on the local time of storm onset, i.e., a given storm will cause effects that are dependent on the longitude of the observing station. Thus, it would be of great interest to

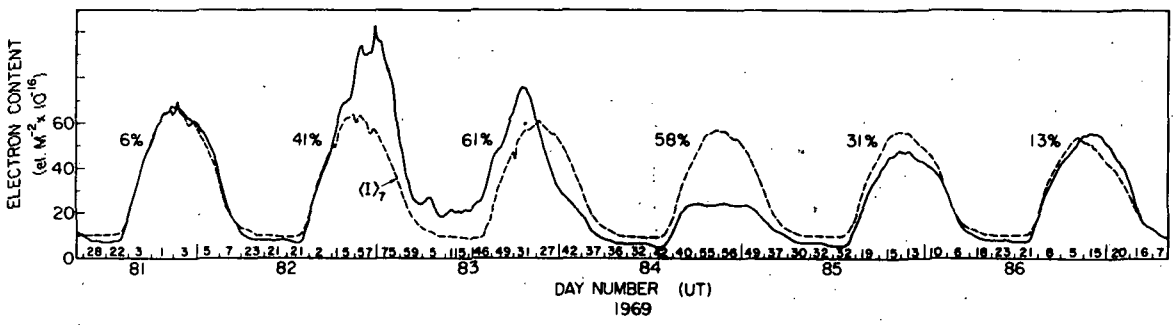

Figure 17. Protonospheric electron content on 14 May 1969, from Stanford. The solid trace curve, I_w, is the observed electron content of the protonosphere. The total slant electron content (dash trace), I, and the universal geomagnetic index, K_p, are also shown. The shaded region in the figure corresponds to the geostationary satellite ATS-3 corrotating in the nightside.

borrow a technique from the geomagnetists and, by using data from a number of equal latitude stations more or less evenly distributed in longitude, expand the storm induced deviation of electron content in a Fourier series in function of longitude:

$$R(\tau) = R_o(\tau) + \sum_n R_n(\tau)\sin[n\ell + \Phi_n(\tau)]$$

where $R = \frac{I - \langle I \rangle}{\langle I \rangle}$

$\langle I \rangle$ is the reference value of electron content,

τ is the time elapsed since the storm onset,

ℓ is the longitude, and

R_n, Φ_n are Fourier coefficients

R_o is independent of longitude and corresponds to D_{st} of geomagnetism.

The behavior of R_o, R_n, and Φ is of great interest to the investigator attempting to uncover the storm producing mechanisms. Unfortunately, at present, there is an insufficient number of electron content observing stations to allow a good determination of these quantities.

If a collection of similar storms, differing only in the universal onset time were available, then one would have an ergodic process and R_o could be calculated from a large number of storms observed at one location rather than from one storm observed from many locations. As individual storms differ greatly from one another such a calculation of R_o yields only their average behavior $\langle R_o \rangle$.

Mendillo[1971] calculated R_o for a total of 28 storms (all with $A_p > 30$) and used the time of the S.C. as the time origin ($\tau = 0$). Figure 18 displays his results and shows clearly the positive, the negative and the recovery phases lasting some 12, 72, and 24 hours respectively.

Although the morphology of storms has been under study for some time, there is room for considerably more investigation based on vast masses of data collected all over the world. A complete study of the

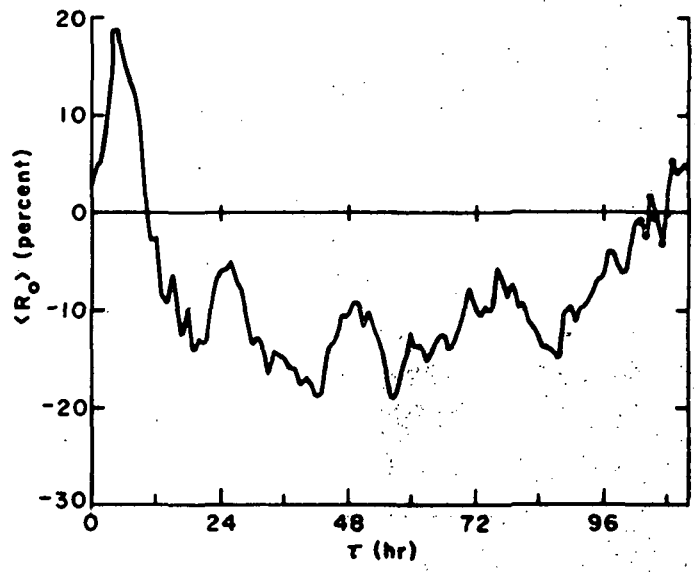

Figure 18. Storm time variation of ionospheric disturbance at midlatitude. From Mendillo[1971].

dependence of this morphology and various factors such as seasons and phases of the solar cycle will without doubt be helpful in building a theory of storms.

Thus, I would like to encourage colleagues all over the world to take part in a comprehensive program of observation of the ionospheric electron content.

ACKNOWLEDGEMENT

The present work was supported by NASA Grant NGR-05-020-001.

REFERENCES

Almeida, O.G., "VHR/UHF technique for the determination of the columnar electron content of the plasmasphere and of the protonosphere using geostationary satellite transmission: Observations during magnetic storms", Tech. Rept. SEL-72-019, Stanford University, 1972.

Almeida, O.G., H. Waldman, and A.V. daRosa, "Neutral winds implied by electron content observations during the 7 March 1970 solar eclipse", J. Atmos. Terr. Phys., 34, 713, 1972.

Bendito, J.L., "The midlatitude ionospheric response to fluctuations in solar activity under low geomagnetic activity conditions", Tech. Rept. SEL-73-023, Stanford University, 1973.

Bent, R.B., S.K. Llewellyn, and M.K. Walloch, "Description and evaluation of the Bent ionospheric model", SAMSO TR-72-239, 1972.

Davis, M.J., "On polar substorms as the source of large-scale traveling ionospheric disturbances", J. Geophys. Res., 76, 4524, 1971.

Garriott, Owen K., "The determination of ionospheric electron content and distribution from satellite observations Part 1. Theory of the analysis", J. Geophys. Res., 65, 1139, 1960.

Herman, J.R., and S. Chandra, "The influence of varying solar flux on ionospheric temperatures and densities: A theoretical study", Planet. Space Sci., 17, 815, 1969.

King, J.W., and H. Kohl, "Upper atmospheric winds and ionospheric drifts caused by neutral air pressure gradients", Nature 4985, 699, 1965.

Klobuchar, J.A., R.S. Allen, "A first-order prediction model of total-electron-content group path delay for a midlatitude ionosphere", Air Force Surveys in Geophysics, 222, AFCRL, 1970.

Mendillo, M., "Ionospheric total electron content behavior during geomagnetic storms", Nature Phys. Sci., 234, 23, 1971.

de Mendonça, Fernando, "Ionospheric electron content and variations measured by Doppler shifts in satellite transmissions", J. Geophys. Res. 67, 2315, 1962.

Rao, N.N., M.Y. Youakim, and K.C. Yeh, "Feasibility study of correcting for excess time delay for transionospheric navigational ranging signals", SAMSO TR-71-163, 1971.

Stubbe, P., "Simultaneous solution of the time dependent coupled continuity equations, heat conduction equations, and equations of motion for a system consisting of a neutral gas, an electron gas, and a four component ion gas", J. Atmos. Terr. Phys., 32, 865, 1970.

Waldman, H., "The coupling between the ionosphere and the protonosphere and its implications on the long-term variations of ionospheric electron content", Tech. Rept. SEL-71-048, Stanford University, 1971.

Waldman, H., and A.V. da Rosa, "Prognostication of ionospheric electron content", Tech. Rept. SEL-71-047, Stanford University, 1971.